Sensors and Materials, Vol. 38, No. 8 (2026) 4859–4872
MYU Tokyo

S & M 4598

Estimation of Backfill Volume by Analyzing Seabed Settlement and Scour Around Offshore Wind Turbine Foundations Using Multibeam Echosounder Data

Jung Hyun Kim,[1] Chan Geun Park,[1] Kyung Jun Kim,[2] and Dong Ha Lee[1*]

[1]Department of Civil Engineering, Kangwon National University,
Kangwondaehak-gil, Chuncheon-si, Gangwon-do 24341, Republic of Korea
[2]Department of Integrated Energy & Infra System, Kangwon National University,
Kangwondaehak-gil, Chuncheon-si, Gangwon-do 24341, Republic of Korea

(Received December 15, 2025; accepted August 10, 2026)

Keywords: hydrographic survey, multibeam echosounder, acoustic sensing, seabed change monitoring, uncertainty assessment, three-dimensional bathymetric model

In offshore wind turbine foundation construction, the seabed settlement induced by pile driving and structural self-weight occurs concurrently with local scour driven by tidal currents, directly affecting foundation stability and backfill design. However, few case studies have quantitatively evaluated construction-stage bed-level changes and verified placed backfill volumes using sensor-derived three-dimensional bathymetric data. In this study, we propose an uncertainty-aware procedure for analyzing seabed settlement and scour and estimating backfill volume at an offshore wind monopile foundation using two-epoch XYZ bathymetric datasets acquired by a USV-mounted multibeam echosounder (MBES) integrated with positioning, attitude, sound velocity, and tidal correction sensors. The two datasets represent conditions after pile driving but before backfilling and after the completion of backfill placement. Grid-based elevation differences (ΔZ) were computed after registering both datasets to a common coordinate system and a 0.25 m grid. A reference seabed surface was introduced to decompose volumetric change into required backfill, actual backfill, and overfill components. Cross-line and reference-zone residuals were also used to define a depth-of-difference uncertainty threshold, preventing changes within measurement uncertainty from being overinterpreted. The case study showed that the most pronounced bed-level changes were concentrated near the monopile. The estimated actual backfill volume was approximately 178.7 m^3, whereas the net volumetric change over the analysis domain was approximately 169.3 m^3. These results demonstrate that MBES-based acoustic sensing and uncertainty-aware XYZ data analysis can support rational backfill design and post-construction performance verification for offshore wind turbine foundations.

1. Introduction

During the construction of monopile foundations for offshore wind turbines, the seabed settlement induced by pile driving and structural self-weight acts in combination with local

[*]Corresponding author: e-mail: geodesy@kangwon.ac.kr
https://doi.org/10.18494/SAM6197

scour generated by currents and waves, causing changes in seabed elevation around the foundation. These changes directly affect foundation stability and backfill-volume planning. Local scour around monopile foundations has been reported to reduce the effective embedment length and lateral stiffness of the foundation and to affect its structural response characteristics.(1,2) Numerous theoretical and experimental studies have investigated the underlying scour mechanisms and associated protection measures.(3,4)

In the early stages of construction, bed-level changes are predominantly governed by settlement due to pile driving and structural self-weight rather than by scour. However, relatively few studies have integrated pre- and post-construction three-dimensional (3D) bathymetric data acquired by multibeam echosounders (MBESs) to jointly resolve settlement and scour components and quantitatively verify placed backfill volume. Although repeat MBES surveys have been used to monitor seabed morphological change and scour-deposition processes in other contexts,(5,6) case studies that jointly quantify settlement, scour, and backfill volume around offshore wind foundations remain scarce.

In this study, we quantitatively characterized seabed settlement and scour behavior and the configuration of backfill deposits around an offshore wind monopile foundation by registering two epochs of MBES-derived XYZ bathymetric data, corresponding to different construction stages, onto a common coordinate system and grid framework and analyzing grid-based bed-level differences. We then proposed an MBES data-driven procedure for rational backfill-volume estimation and post-construction performance verification.

From the viewpoint of sensing applications, the MBES does not merely provide a visual representation of seabed topography. It functions as an active acoustic sensing system that converts construction-stage seabed morphology into high-density georeferenced XYZ observations when combined with global navigation satellite system (GNSS), inertial attitude measurements, sound velocity profiles, and tidal correction data. Therefore, the reliability of the derived volumetric indicators depends on both acoustic measurement performance and uncertainty management during data processing.

Because the volume calculation is based on the depth of difference (DoD) between two survey epochs, small vertical or horizontal registration errors can propagate directly into the estimated backfill volume. Accordingly, this study explicitly considers residuals from cross-line checks, stable reference zones, and grid-node variability when interpreting ΔZ and volumetric components, rather than treating all centimeter-scale differences as physical seabed change.

The study site surrounds a single monopile foundation within an offshore wind farm located off Nakwol-myeon, Yeonggwang-gun, Jeollanam-do, Korea. The analysis domain was defined to focus on the area where pile installation and subsequent backfilling were conducted. It was delineated as a circular area centered on the pile with a prescribed radius to capture both concentrated settlement in the immediate vicinity of the foundation and more gradual morphological changes in the outer zone. The bathymetric data include MBES observations processed into XYZ format after applying sound velocity, attitude, and positioning corrections. Two survey epochs were used: one after pile driving and before backfilling and the other after the completion of backfill placement.

The two datasets were reconstructed using an identical horizontal coordinate system, depth datum, and grid spacing, and the pre- and post-construction bed surfaces were compared to evaluate bed-level changes and estimate backfill volume. The scope of this study is confined to observation-based 3D seabed morphology analysis and volumetric assessment; the numerical modeling of long-term scour and sedimentation processes is beyond the present scope. The study location and analysis domain are presented in Fig. 1. Uncertainty propagation and reference-surface sensitivity are discussed explicitly to clarify the reliability and limitations of the proposed workflow.

2. Methods

The methods used comprise survey instrumentation, environmental and motion corrections, noise and outlier removal, data registration, 3D bathymetric modeling, volumetric decomposition, and uncertainty assessment.

2.1 Survey instrumentation

A small unmanned surface vessel (USV) equipped with a Sonic™ 2020-V MBES manufactured by R2 Sonic was used to acquire high-resolution seabed topography around the offshore wind turbine foundation. The multibeam system includes a high-frequency transmit/receive unit, an underwater mounting frame, and integrated control and data-acquisition software. It transmits 1024 beams over a 10–130° swath, and the final bathymetric products were

Fig. 1. (Color online) Study site and analysis domain around the offshore wind turbine monopile foundation.

generated on a 0.25 m grid. MBES instruments of this type have become standard for the high-resolution imaging of seabed morphology and sedimentary structures in coastal and shelf environments.[7] Recent studies have also incorporated uncertainty-prediction models that explicitly account for system components and environmental conditions when assessing depth-measurement accuracy.[8] In this study, the MBES, GNSS, inertial sensor, sound velocity profiler, and tidal correction data were treated as an integrated sensing chain because the final bathymetric grid and volumetric products inherit uncertainty from each component.

The sonar head was rigidly mounted at the center of the vessel keel to minimize beam-direction changes associated with vessel motion. Time stamps, positions, and attitude corrections from an external GNSS receiver and an inertial measurement unit (IMU) were synchronized with the acquisition system to ensure the positional and attitude accuracy of the acoustic soundings.

The survey platform is a catamaran-type USV with a compact hull and electric propulsion system designed for stable navigation and precise path following in shallow water. Repeated cross-lines around the pile can be run within the restricted work area at nearly constant speed and line spacing using remote-control and autonomous-navigation modes. Similar MBES-equipped unmanned surface platforms have been proposed as efficient and safe hydrographic survey tools for shallow and otherwise hard-to-access coastal environments.[9] The present configuration emphasizes the acquisition of consistent 3D bathymetric datasets for the same area before and after construction, which were subsequently used as XYZ-format base data for seabed-level change analysis and backfill-volume estimation. Table 1 shows the principal MBES specifications, and Table 2 shows the USV specifications. Comparable configurations combining MBES with auxiliary positioning and attitude sensors have been widely used for routine seabed-mapping surveys along the Korean coast.[10] The present setup applies this established hydrographic practice to offshore wind turbine foundations.

Table 1
(Color online) Specifications of Sonic™ 2020-V MBES.

Manufacturer	R2 Sonic
Model	Sonic™ 2020-V
Frequency range	200–450 kHz
Number of beams	1024
Maximum survey depth	200 m
Swath angle	10–130°
Beam footprint	1.8° × 1.8° at 450 kHz
	4° × 4° at 200 kHz

Table 2
Specifications of USV.

Dimensions ($W \times L \times H$)	1016 × 1475 × 457.3 mm^3
Power system	LiPo batteries, 22.2 V, 22000 mAh × 8 (2 sets)
Communication	RF and LTE
Internal electronics power	24 V inverting system
Installable sensors	SBES and MBES
Main functions	RTK-based autopilot

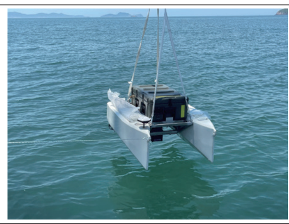

2.2 Sound velocity and tidal corrections

Sound velocity correction was conducted using both vertical sound velocity profiles and continuously observed sound velocity data acquired in the field. The vertical sound velocity structure was periodically measured at representative stations within the survey area, and additional profiles were collected along long transit sections to capture temporal and spatial variability.

The acquired sound velocity profiles were applied in the hydrographic data-processing software for recomputing beam paths and correcting refraction errors associated with the beam angle. For outer, high-angle beams in which refraction effects were pronounced, the quality class was deliberately downgraded so that such beams can be selectively excluded in subsequent filtering stages.

Tidal correction was performed using a tide model constructed from long-term water level records at the Yeonggwang tidal station. The water level at each survey time was estimated from the tide model and converted to a common vertical reference (datum level). Then, the corresponding correction values were applied to the depth soundings to reduce all depths to a consistent vertical datum.

When applying the tide model, periods in which rapid water-level changes or anomalous values were expected were examined by comparison with observed tides to examine error tendencies, and, where necessary, deviations in the correction were adjusted to mitigate the effect of local spikes.

After applying sound velocity and tidal corrections, residuals in crossing lines and nominally flat seabed areas were examined in terms of mean, standard deviation, and dependence on the depth and beam angle to identify under- or over-correction tendencies. When required, the choice of sound velocity profiles and the manner of applying the tide model were revised such that a consistent-datum depth dataset can be used in the subsequent registration and modeling stages. These preprocessing steps serve to jointly manage system- and environment-related error sources in the MBES measurements and keep depth uncertainties within acceptable bounds, which is in line with the concept of recently proposed MBES uncertainty-prediction models.[(8)]

2.3 Noise and outlier removal

Noise and outlier removal was conducted by combining line-based editing and spatial-based editing. In the line-based editing stage, quality indices provided by the MBES system, such as received amplitude, beam angle, and quality flags, were used to preferentially remove spike-type outliers, i.e., depth values that deviated abnormally from neighboring pings within the same line. High-angle beams on the outer edge of the swath and segments with unstable echo waveforms were also excluded.

In the subsequent spatial-based editing stage, local planes or low-order surfaces were fitted within blocks or grid cells of specified size. Points with excessively large residuals from these fitted surfaces were classified as outliers and removed, and areas with a large variance within the same cell were assigned lower reliability so that their effect would be reduced during later interpolation.

The data systematically distorted by observational conditions, such as acoustic shadowing, multipath, and passage through bubble plumes, were masked and removed in bulk. Low-frequency undulations arising from imperfect heave correction were mitigated by combining a high-pass (low-cut) filter with a moving-median filter.

Following filtering, removal rates, depth histograms, and residual distributions were compared to verify that the intrinsic seabed morphology and scour–backfill boundary around the foundation had not been excessively smoothed. In segments where the outlier removal ratio was abnormally high, survey tracks and field conditions were reviewed together, and supplementary survey data were incorporated where necessary. Through this procedure, observational noise and obvious outliers were eliminated selectively, while the actual seabed configuration and characteristics of bed-level change were preserved as much as possible.

2.4 Data registration

Data registration is a key step for directly comparing the two MBES datasets acquired before and after construction within a common horizontal and vertical reference frame and is therefore essential for analyzing seabed-level changes and estimating backfill volume.

Using the results of sound velocity, tidal, motion, and positioning corrections applied separately to each survey epoch, the horizontal positions were first transformed into a common map projection, and the depth values were reduced to a common vertical datum. Through this process, the basic reference frames of the two datasets were unified.

Within the overlapping survey area around the foundation, the pre-construction (pre-backfill) bathymetric surface was defined as the reference model. Rigid-body translation parameters in horizontal and vertical directions were subsequently estimated for the post-construction (post-backfill) model. To this end, reference zones commonly covered in both surveys, such as clearly defined structural elements (e.g., exposed portions of the foundation) and relatively flat seabed areas assessed to be minimally affected by backfilling, were selected. Translation parameters were iteratively adjusted to minimize the mean and systematic bias of depth differences between the two epochs within these reference zones.

Where necessary, small rotation terms were considered to alleviate local slope discrepancies and residuals arising from attitude correction; however, the degrees of freedom of the transformation were kept to the minimum required to avoid the artificial distortion of the actual seabed morphology.

The registration results were verified by examining the distribution of residuals in the reference zones, trends of depth differences with respect to depth and planimetric location, and cross-sectional comparisons along and across the survey lines. The registration parameters were refined until the mean residuals approached zero and the standard deviation and spatial pattern of the residuals fell within acceptable limits.

Through this procedure, the two MBES datasets from different epochs were consistently superposed within a common reference frame, reducing the registration error in the subsequent grid-based analysis of seabed-level changes and in the estimation of backfill volume. Such a unification of reference frames and an explicit management of registration error are essential for reliably evaluating seabed-change magnitudes from repeat MBES surveys. The importance of uncertainty assessment in DoD-based volumetric calculations has been highlighted in previous studies.(5,8)

2.5 Construction of 3D bathymetric model

The 3D bathymetric model was constructed by converting the preprocessed, corrected, and co-registered MBES point clouds to a regular grid with a specified spacing. For the pre- and post-construction point clouds, the horizontal resolution was set to 0.25 m considering the sounding density in the vicinity of the foundation and scale of seabed-morphology changes, and the same grid system was applied to both epochs when assigning depth values.

For each grid cell, the representative depth was computed as a weighted average of neighboring soundings, considering the vertical variance and number of observations. Points classified as outliers in the previous filtering stage were removed in advance so that their effect would not be reflected in the gridded depths. In boundary zones and acoustic-shadow regions where data were sparse, missing cells were filled by interpolating the trend of the surrounding grid cells. For the upper surfaces of fixed structures and reference topography where the effect of backfilling and settlement was negligible, separate masks were applied so that the model geometry would remain as close as possible to the original shape.

The resulting pre- and post-construction 3D bathymetric models were visualized as TIN surfaces, depth contours, and shaded-relief maps to examine seabed characteristics around the foundation. These gridded models were also used to compute grid-based bed-level differences and estimate backfill volume. The high-resolution models provide a practical means of visualizing seabed morphology and scour patterns and can be used for the long-term monitoring of seabed-level changes around offshore wind turbine foundations.(6,7,10) The pre- and post-construction 3D bathymetric models are shown in Fig. 2.

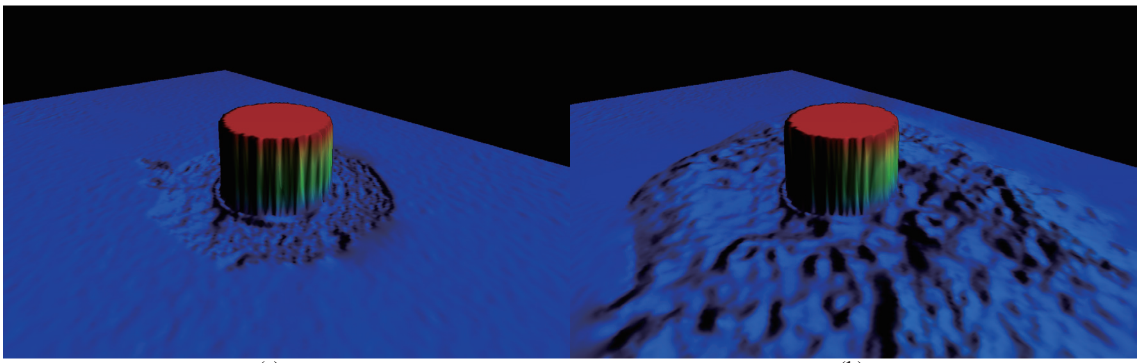

(a) (b)

Fig. 2. (Color online) Pre- and post-construction 3D bathymetric models around the foundation. (a) Pre-backfill surface after pile driving. (b) Post-backfill surface after placement. Color gradation indicates relative bed elevation, with blue representing lower seabed areas and red representing higher topography around the monopile.

2.6 Analysis of seabed-level change and backfill-volume estimation

The bathymetric models were compared to quantify bed-level changes and the resulting volumes were decomposed according to the proposed framework.

The pre- and post-construction 3D bathymetric models were compared on a common grid to analyze the seabed-level change around the monopile foundation. For each grid cell i within the analysis domain, the bed-level difference ΔZ_i was defined as

$$\Delta Z_i = Z_{post,i} - Z_{pre,i} \, , \tag{1}$$

where $Z_{pre,i}$ represents the bed level (or reference water depth) of cell i in the pre-backfill bathymetry representing settlement and initial scour after pile driving, and $Z_{post,i}$ represents the bed level in the post-backfill bathymetry. A negative ΔZ_i indicates an additional lowering of the seabed between the two epochs, whereas a positive ΔZ_i indicates a net increase in bed level attributable to backfill placement.

The ΔZ distribution shows that changes on the order of 10^{-2} m are widespread throughout the analysis domain, whereas changes on the order of 10^{-1} m are concentrated near the monopile. A reference seabed surface, Z_{ref}, was introduced to interpret these changes consistently in terms of settlement/scour and backfill.

The reference seabed surface was defined on the basis of the mean water depth and relief characteristics of outer natural seabed zones judged to be minimally affected by the foundation and backfilling. A representative seabed surface was estimated and extrapolated over the entire analysis domain using these outer zones. This surface is interpreted as an approximation of the original seabed prior to pile installation and construction, and it is used as a baseline to evaluate voids generated by settlement and scour and the effect of backfill placement.

Comparing the pre-backfill bathymetry with the reference seabed surface shows that, in the immediate vicinity of the pile, $Z_{pre,i}$ is smaller (deeper) than $Z_{ref,i}$, forming continuous depressions below the reference seabed. These depressions are interpreted as cavities produced by settlement because of pile driving and structural self-weight, combined with local scour. After backfilling, $Z_{post,i}$ approaches or exceeds $Z_{ref,i}$ near the foundation, indicating that these depressions are largely filled, and in some areas, embankment-type deposits higher than the reference seabed have formed. Toward the outer boundary of the analysis domain, ΔZ_i approaches zero and the seabed morphology remains similar to the natural seabed.

2.7 Decomposition of backfill volume

The volumetric change around the foundation can be decomposed into (i) the required backfill volume to fill settlement/scour-induced voids, (ii) the actual backfill volume, and (iii) the overfill volume above the reference seabed by introducing the reference seabed surface. Let A denote the area of one grid cell; in this study,

$$A = 0.25\text{ m} \times 0.25\text{ m} = 0.0625\text{ m}^2. \quad (2)$$

The required backfill volume V_{req} is defined as the volume between the reference seabed surface and the pre-backfill bathymetry, computed only where settlement and scour have lowered the seabed below the reference seabed.

$$V_{req} = \Sigma_i \max(0, Z_{ref,i} - Z_{pre,i})A \quad (3)$$

Here, the operator max(0, ·) sets the contribution to zero where the seabed is at or above the reference surface ($Z_{ref,i} \leq Z_{pre,i}$), thereby integrating only the volume of newly formed depressions relative to the original seabed. This volume represents the theoretical backfill volume required to restore the seabed to the reference level.

The actual backfill volume V_{fill} is defined as the integral of positive bed-level changes between the pre- and post-backfill bathymetry.

$$V_{fill} = \Sigma_i \max(0, Z_{post,i} - Z_{pre,i})A \quad (4)$$

V_{fill} includes both the volume used to fill the settlement/scour depressions and the volume that raised the seabed above the reference seabed. In other words, V_{fill} represents the net additional volume of material placed by backfilling between the two survey epochs.

The overfill volume V_{over} is defined as the volume between the reference seabed surface and the post-backfill bathymetry, where the latter is higher than that of the reference seabed.

$$V_{over} = \Sigma_i \max(0, Z_{post,i} - Z_{ref,i})A \quad (5)$$

Thus, cells satisfying $Z_{post,i} > Z_{ref,i}$ represent zones where backfill has formed an embankment higher than the reference seabed. The corresponding volume V_{over} can be interpreted as overfill in excess of the theoretically required backfill volume V_{req}.

Using these definitions, we can evaluate the volumetric change around the foundation from three complementary perspectives: (i) the void volume generated by settlement and scour relative to the reference seabed (V_{req}), (ii) the net actual backfill volume between the two survey epochs (V_{fill}), and (iii) the overfill volume above the reference seabed after backfilling (V_{over}).

This decomposition framework provides a quantitative basis to compare design-stage backfill volume with as-built conditions and assess the adequacy of backfill thickness and extent from the viewpoint of both stability and construction efficiency.

2.8 Uncertainty assessment and reference-surface sensitivity

Because the proposed volume calculation is based on DoD analysis, uncertainty was evaluated before interpreting the spatial distribution of bed-level change. The principal error sources considered in this study were MBES range and beam-angle uncertainty, sound velocity correction, heave/roll/pitch/yaw compensation, GNSS positioning, tidal reduction, interpolation to a regular grid, and the residual registration error between the two epochs. Modern hydrographic standards and recent NOAA specifications emphasize that gridded bathymetric products should retain node-wise depth and uncertainty information, for example, through CUBE-type gridding or Bathymetric Attributed Grid products.[(11–13)]

For each grid node i, the standard uncertainty of the DoD was expressed as $\sigma(\Delta Z,i) = [\sigma(\text{pre},i)^2 + \sigma(\text{post},i)^2 + \sigma(\text{reg})^2]^{1/2}$, where $\sigma(\text{pre},i)$ and $\sigma(\text{post},i)$ are the vertical uncertainties of the pre- and post-backfill surfaces, respectively, and $\sigma(\text{reg})$ is the residual uncertainty associated with co-registration. The 95% limit of detection was defined as $\text{LoD}(95,i) = 1.96\sigma(\Delta Z,i)$. Changes satisfying $|\Delta Z| \leq \text{LoD}(95,i)$ were treated as statistically indistinguishable from zero, whereas changes exceeding this threshold were interpreted as meaningful seabed lowering or backfill placement.

The corresponding uncertainty of a volume component V was propagated as $\sigma(V) = A[\Sigma_i\sigma(\Delta Z,i)^2]^{1/2}$, where A is the grid-cell area and the summation is taken over the cells included in each volume calculation. The resulting confidence interval can be expressed as $V \pm 1.96\sigma(V)$. In the present case, the archived XYZ datasets did not include full node-wise CUBE uncertainty metadata; therefore, $\sigma(\text{pre},i)$ and $\sigma(\text{post},i)$ were estimated from cross-line residuals, stable outer-zone residuals, and local grid variance after outlier removal. This limitation is explicitly considered when interpreting small-magnitude changes.

The sensitivity of the required backfill volume and overfill volume to the reference seabed surface was examined by redefining the outer natural seabed zones used to estimate Z_{ref} and by comparing the resulting spatial patterns of Vreq and Vover. The actual backfill volume V_{fill}, which is computed directly from the positive ΔZ between the two survey epochs, is less sensitive to the assumed reference surface; in contrast, V_{req} and V_{over} should be interpreted together with the uncertainty and sensitivity of Z_{ref}.

3. Results

In this section, we discuss the spatial characteristics and results of the quantitative evaluation.

3.1 Spatial characteristics of bed-level change around the monopile

Using the co-registered pre- and post-construction 3D bathymetric models with a grid spacing of 0.25×0.25 m^2, the bed-level difference ΔZ values were computed for all grid cells within the analysis domain. The resulting distribution shows that changes on the order of 10^{-2} m are widespread throughout the domain, whereas those on the order of 10^{-1} m are concentrated in the vicinity of the monopile foundation.

In the plan view, the zone of the pronounced bed lowering and subsequent recovery appears as an approximately circular pattern centered on the pile, with locally steeper gradients in the immediate vicinity of the foundation and more gradual transitions toward the outer boundary of the analysis area. The histogram of ΔZ_i is slightly skewed toward positive values, which reflects the dominance of bed-level increase because of backfill placement over the additional lowering that occurred between the two survey epochs. However, the magnitude of negative ΔZ_i near the pile confirms that part of the settlement and scour continued after the first survey epoch, even within the short construction interval considered in this study.

3.2 Quantitative evaluation of settlement/scour, backfill, and overfill volumes

On the basis of the reference seabed surface $Z_{ref,i}$ defined from the outer natural seabed zones, the volumetric components introduced in the previous section were evaluated on the common grid. The grid-cell area was $A = 0.25\text{ m} \times 0.25\text{ m} = 0.0625\text{ m}^2$.

First, the volume corresponding to negative bed-level changes between the pre- and post-construction bathymetry ($\Delta Z_i < 0$) was interpreted as the additional settlement/scour volume that developed during the interval between the two surveys. This volume, obtained by integrating $\Delta Z_i A$ over cells with $\Delta Z_i < 0$, was approximately 9.4 m³, which indicates that a limited amount of further bed lowering occurred after the pre-backfill survey.

The actual backfill volume V_{fill} was defined as

$$V_{fill} = \Sigma_i \max(0, Z_{post,i} - Z_{pre,i})A. \tag{6}$$

The actual backfill volume was approximately 178.7 m³ for cells with $\Delta Z_i > 0$. This represents the net additional volume of the material placed during backfilling between the two survey epochs, including the volume required to fill the settlement/scour depression and the volume that raised the seabed above the reference seabed.

The net volume change over the entire analysis domain was computed as

$$V_{net} = \Sigma_i \Delta Z_i A. \tag{7}$$

The net volume change was approximately 169.3 m³, which is smaller than V_{fill} because it includes the effect of additional settlement/scour (negative ΔZ_i) as well as infilling (positive ΔZ_i).

Using the reference seabed surface, the required backfill volume to restore the seabed to the reference level can be expressed as

$$V_{req} = \Sigma_i \max(0, Z_{ref,i} - Z_{pre,i})A, \tag{8}$$

where only cells with $Z_{ref,i} < Z_{pre,i}$ are integrated. Although the exact numerical value of V_{req} depends on how $Z_{ref,i}$ is defined, the comparison of spatial patterns shows that the post-backfill bed level $Z_{post,i}$ is higher than $Z_{ref,i}$ in many cells around the pile.

The corresponding overfill volume V_{over} is defined as

$$V_{over} = \Sigma_i \max(0, Z_{post,i} - Z_{ref,i})A. \tag{9}$$

This represents the volume of the material placed above the reference seabed surface. Qualitatively, V_{over} is concentrated in zones adjacent to the monopile where the seabed is intentionally raised to form a slightly elevated backfill mound relative to the surrounding natural seabed.

In the uncertainty-aware interpretation, widespread bed-level changes on the order of 10^{-2} m in the outer part of the domain were treated cautiously because they may fall within the combined DoD uncertainty. By contrast, the changes on the order of 10^{-1} m concentrated around the monopile exceeded the expected uncertainty envelope and were therefore interpreted as construction-related settlement, scour, and backfill morphology.

The reference surface sensitivity check showed that V_{fill} and the net volumetric change are controlled mainly by the direct difference between the two MBES surfaces, whereas V_{req} and V_{over} vary with the assumed Z_{ref}. Therefore, V_{req} and V_{over} are most useful as construction-management indicators when the reference seabed surface is defined consistently across foundations and survey campaigns.

4. Discussion

The pre-backfill bathymetry exhibited a distinct depressed area around the pile relative to the reference seabed surface, which suggests that settlement and initial scour produced a continuous depression rather than isolated scour holes. After backfilling, the post-construction bathymetry showed that this depression was largely infilled and that the seabed around the monopile was raised toward or slightly above the reference seabed surface. In some sub-areas adjacent to the foundation, the post-backfill bed level exceeded that of the reference seabed, forming a low embankment-type morphology. From a design and construction-management perspective, this suggests that the backfill placement was conducted conservatively in terms of thickness and spatial extent to secure foundation stability and provided a margin against future scour, albeit at the cost of the increased backfill volume relative to the minimum theoretical requirement.

At the outer edge of the analysis domain, ΔZ values were close to zero and the seabed morphology remained comparable to the natural seabed, suggesting that the direct effect of backfill placement was spatially confined around the foundation. In the analyzed case, the backfill operation not only compensated for the settlement/scour-induced depression but also produced a certain degree of overfilling around the foundation. For offshore wind monopile foundations, intentional overfilling with rock or sand can provide a safety margin against future scour and stiffness loss, consistent with the common design and construction strategies reported in the literature.(1,2) These findings can also be interpreted in light of existing theoretical and experimental studies on scour mechanisms and scour-protection measures.(3,4)

The uncertainty assessment clarifies that the main volumetric conclusion does not depend on interpreting every small ΔZ value as physical change. The estimated actual backfill volume of approximately 178.7 m^3 was derived from positive changes between the two co-registered MBES surfaces, whereas the net volumetric change of approximately 169.3 m^3 reflects both positive backfill placement and negative residual settlement/scour. This distinction prevents the additional settlement from being obscured within a single net-volume value.

The sensitivity of the reference seabed surface is also important. If Z_{ref} is defined slightly higher, both the required backfill volume and overfill volume increase; if it is defined slightly lower, both values decrease. However, the spatial interpretation remains stable when the same outer natural seabed zones are used because the largest positive and negative changes are concentrated near the monopile rather than along the analysis boundary. The proposed framework is therefore robust for relative construction-stage verification, although absolute values of V_{req} and V_{over} should be reported together with the criteria used to define Z_{ref}.

The broader applicability of the workflow depends on the standardizing survey design, grid spacing, vertical datum, uncertainty metadata, and reference-surface definition across multiple foundations and survey epochs. For future projects, exporting node-wise uncertainty using CUBE/BAG-type products and applying a consistent DoD limit of detection would facilitate a direct comparison among foundations and improve the method for long-term monitoring and construction quality control.[11–15]

5. Conclusions

In this study, we presented a procedure for analyzing seabed-level change and estimating backfill volume around an offshore wind turbine monopile foundation using two epochs of MBES data. A key feature is the introduction of a reference seabed surface derived from outer natural seabed zones with a minimal construction effect. Using this surface as a baseline, volumetric change was decomposed into (1) the required backfill volume associated with voids generated by settlement and scour relative to the reference seabed, (2) the actual backfill volume between the two survey epochs, and (3) the overfill volume representing deposits above the reference seabed after backfilling. This framework provides a physically interpretable basis for linking observed bed-level changes to backfill design and construction practice.

The case study indicated that changes on the order of 10^{-2} m were widespread over the analysis domain, whereas those on the order of 10^{-1} m were concentrated near the monopile. The depression formed around the foundation after pile driving was largely infilled by backfilling. In some areas, the post-construction bed level exceeded the reference seabed and formed a low backfill mound. The estimated actual backfill volume exceeded the additional settlement/scour volume between the two survey epochs, and the spatial distribution of overfill indicated that backfill was placed conservatively in terms of thickness and extent to enhance foundation stability and scour resistance.

The proposed MBES-based method can be used to compare design-stage backfill volume with as-built conditions and evaluate the adequacy of the backfill configuration. From a sensing-application perspective, the study demonstrates how MBES acoustic measurements, positioning and attitude sensors, sound velocity observations, and tidal correction data can be integrated into a quantitative construction-verification workflow. DoD uncertainty propagation helps distinguish meaningful seabed change from measurement and registration noise, thereby improving the reliability of volume estimates.

This study is limited to a single foundation and a single pair of survey epochs, and the quantitative values of required and overfill volumes depend on the definition of the reference seabed surface. In addition, the archived XYZ datasets did not contain complete node-wise CUBE/BAG uncertainty metadata; therefore, uncertainty was assessed from residual statistics and grid variability rather than from full per-node hydrographic uncertainty records.

Future work should include repeated MBES surveys of multiple foundations to construct time series of seabed-level changes and coupling with numerical models to examine relationships among flow conditions, scour development, and backfill behavior. Standardized procedures for defining the reference seabed surface, retaining node-wise uncertainty metadata, and systematically compiling differences between design and as-built backfill volumes will contribute to data-driven guidelines for backfill design and construction quality control in offshore wind turbine foundation projects.

Acknowledgments

This work was supported by the National Research Foundation of Korea (NRF) grant funded by the Korea government (MSIT) (IRIS RS-2024-00350440).

References

1 H. Qu, H. An, S. Draper, P. Watson, M. Zhao, J. Harris, R. J. S. Whitehouse, and D. Zhang: Ocean Eng. **301** (2024) 117385. https://doi.org/10.1016/j.oceaneng.2024.117385
2 J. E. Saathoff, N. Goldau, M. Achmus, A. Schendel, M. Welzel, and T. Schlurmann: Appl. Ocean Res. **144** (2024) 103920. https://doi.org/10.1016/j.apor.2024.103920
3 B. M. Sumer and J. Fredsøe: The Mechanics of Scour in the Marine Environment (World Scientific, Singapore, 2002).
4 M. Wei, X. Wang, M. Li, J. Li, H. Fang, and Z. Huang: Renew. Sustain. Energy Rev. **182** (2024) 113524. https://doi.org/10.1016/j.rser.2023.113524
5 A. C. G. Schimel, D. Ierodiaconou, M. Hulands, and D. Kennedy: Cont. Shelf Res. **111** (2015) 52. https://doi.org/10.1016/j.csr.2015.10.019
6 H. Zheng, T. Zhu, Z. He, and Y. Qi: South. Energy Constr. **10** (2023) 88.
7 J. E. Hughes Clarke, L. A. Mayer, and D. E. Wells: Mar. Geophys. Res. **18** (1996) 607. https://doi.org/10.1007/BF00313877
8 M. R. Mohammadloo, M. Snellen, and T. J. Simons: Appl. Sci. **10** (2020) 4671. https://doi.org/10.3390/app10134671
9 B.-C. Kum, D.-H. Shin, S. Jang, S. Y. Lee, J. H. Lee, T. J. Moh, D. G. Lim, J.-D. Do, and J. H. Cho: J. Coast. Res. **95** (2020) 1152.
10 H. D. Kim, S. Aoki, K. H. Kim, J. Kim, B. Shin, and K. Lee: J. Coast. Res. **95** (2020) 527.
11 B. R. Calder and L. A. Mayer: Geochem. Geophys. Geosyst. **4** (2003) 1048. https://doi.org/10.1029/2002GC000486
12 International Hydrographic Organization: IHO Standards for Hydrographic Surveys, S-44 (IHO, Monaco, 2024) 6th ed. https://doi.org/10.25607/OBP-388.4
13 National Oceanic and Atmospheric Administration: Hydrographic Surveys Specifications and Deliverables (NOAA Office of Coast Survey, Silver Spring, MD, 2025) https://www.nauticalcharts.noaa.gov/publications/documents/HSSD_2025-0-01.pdf (accessed August 2026).
14 R. J. S. Whitehouse: Scour at Marine Structures (Thomas Telford, London, 1998).
15 C. Matutano, V. Negro, J.-S. López-Gutiérrez, and M. D. Esteban: Renew. Energy **57** (2013) 358. https://doi.org/10.1016/j.renene.2013.01.032